Journal of
Software
Engineering

Academic
Journals Inc.

CrossMark

Research Article
Dynamic Modeling of the Human-Computer Interaction for Upper Limb Rehabilitation Robot

Xing Li and Xiaofeng Wang

State Key Laboratory of Synthetical Automation for Process Industries, Northeast University, 110004 Shenyang Liaoning Province, China

Abstract

Background: A lot of machines have been developed for the upper-limb rehabilitation to meet the patient's needs of upper-limb rehabilitation exercises. As active exercise has been proven to be effective and necessary for neural rehabilitation and motor recovery, it is suggested to be implemented to the rehabilitation machines. To get this goal, the human motion's desire should have been recognized exactly first. Because the muscle strength of the patient's upper limb may not be able to supply the gravity of the arm and the rehabilitation machines, some torques comes from the rehabilitation machines will be needed to supply the exercise. **Materials and Methods:** This study is focused on modeling and identifying the human-computer interaction dynamics, so that the motion's desire is able to be recognized exactly based on it. Firstly, the human upper limb can be taken as two links with three degrees of freedom (two DOF in shoulder, one in elbow). By combining the dynamics model of human upper limb and robot, the human-computer interaction dynamic model was formed. **Results:** Meanwhile, the joint angles and torques of human upper limb be measured indirectly by using the position and torque sensors mounted on the joints of the exoskeleton. **Conclusion:** In this way, a 19 parameter human-computer interaction dynamic model has been established by using the Lagrange method based on the pseudo inertia matrix. The feasibility of the human-computer interaction dynamic model is validated by comparing the math model to the simulation model established by the SolidWorks and the Sim Mechanics.

Competing Interest: The authors have declared that no competing interest exists.

Data Availability: All relevant data are within the study and its supporting information files.

INTRODUCTION

Stroke is one of the higher incidences of the disease in the elderly. The motor dysfunction which is caused by the stroke has a serious impact on the health of older people[1]. The traditional methods for upper limb rehabilitation usually needs the physicians trait the patients one to one and one by one[2,3]. It is inefficient and impose heavy burden on the family and society. Proper rehabilitation exercise training can promote the recovery of the physical activity function for the patients[4]. The exercise training of upper limb rehabilitation assisted by the robot is more targeted, longer lasting and repeatable. Several studies have shown that robot-aided rehabilitation has much better significant than traditional method[5,6]. Therefore, more and more attentions have been paid to the upper limb rehabilitation robot[7], which was supposed to be able to free the physicians out of the heavy manual works, improve the efficiency of rehabilitation and meanwhile reduce the burden of the associated people[8,9]. Figure 1 shows, the training system of the 5 DOF exoskeleton robot[10] for upper limb rehabilitation, is a medical device which is used to serve the patients with hemiplegic upper limb and assist the physician to complete the rehabilitation. This system can accomplish large-scale single joint movement or multi-joint compound movement and realize the patient's motion of daily activities. It consists of two parts: The exoskeleton mechanical structure and the control system. The mechanical structure has five degrees of freedom, which are shoulder elevation, shoulder roll, elbow flexion/extension, wrist roll and wrist flexion/extension. The base part and five irregular rigid links are connected together by the movable joints; each joint is driven by a motor. The orientation of each joint between two parts is also inconsistent in the triaxial X-Y-Z coordinates system. The rotation angle of each joint also has certain limitations considering the security of rehabilitation.

In the exercises provided by the exoskeleton, the angular range of the wrist joint is relatively small and has little effect on the dynamics; therefore, the wrist joint is neglected in the modeling[11] and keep the wrist joint unchanged during the simulation experiment. Then the exoskeleton for upper limb rehabilitation can be regarded as an irregular exoskeleton machine which has 3 DOF. The inertia properties should be described by pseudo inertia matrix in the dynamic model[10,12]. To insure the range of exercises and match the motion of the exoskeleton, the wrist's motion of human arm were neglected similarly. The human arm can be seen as a manipulator with two links and 3 DOF in the modeling of dynamics.

Fig. 1: Training system of the 5 DOF exoskeleton robot for upper limb rehabilitation

For the measurement of the joint torques, there was a method[13,14] that using torque sensors mounted on the end effecter of the exoskeleton to measure some values and then convert them to the joint torques by the Jacobian matrix. This method will not only impose additional constraints on the patients' hand but also get a converted data which may be not able to reflect the real joint torques. In fact, if the Human Upper Limb (HUL) is bound on the exoskeleton, the rotation centers of the exoskeleton's joints can be consistent with HUL by adjusting the length of the links. The angle's change on each joint of HUL and the exoskeleton will be the same, they are all can be measured directly by the sensors mounted on the exoskeleton and the joint torques of HUL can be obtained indirectly from the joint torque sensors mounted on the joints of the exoskeleton.

Active exercise is considered more effective than the passive one for the motor recovery of the upper limb[15]. In order to realize active rehabilitation exercise, the voluntary motion desire of the patients should be recognized. It has been carried out by using the electromyography (EMG) in the literature[16,17]. However, every single patient is in different situation, the EMG signals are different from person to person and the accuracy of EMG is affected by a lot of factors. So, it would take a complex and repeated debugging before it was used to the patient.

Based on this study, the dynamics parameters are identified based on the sensors mounted on every joint of the exoskeleton and are used to recognize the human motion desire. This method reduces the use of the external device and avoids the interference of external factors. The measured data is more stable and reliable and the result of identification and
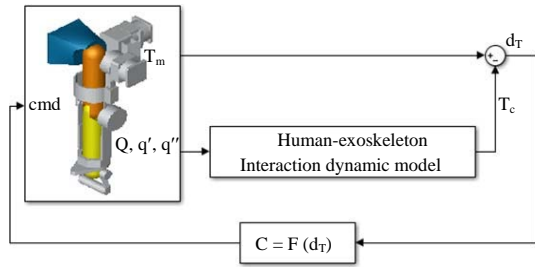
Fig. 2: Structure of the human motion desire recognized in active rehabilitation exercise

recognition is more accurate. Figure 2 depicts the structure of recognizing the human motion desire by human-computer interaction dynamics in active rehabilitation exercise. The angles and torques in Fig. 2 are measured by the sensors mounted on the joints of the exoskeleton.

It can be seen from Fig. 2 that T_m is the measured torques and T_c is calculated from human-computer interaction dynamics. The d_T represents the human motion desire. When d_T is less than zero, it shows that HUL has imposed a torque in the direction of movement and the motion desire is towards the positive orientation. Otherwise if d_T is greater than zero, it means HUL has imposed a torque against the direction of movement and the motion desire is towards the negative orientation. If d_T equals to zero, there is no additional torques and no motion desire. A threshold value of d_T can adjust the sensitivity. The control commands[18] can be derived from d_T.

MATERIALS AND METHODS

Modeling of the exoskeleton and the human upper limb
Modeling of exoskeleton: Figure 3 shows that, the D-H method[19] is used in the kinematics modeling of the exoskeleton and the D-H parameters are given in Table 1. The Lagrange method is used to model the dynamics of the exoskeleton, which is defined by the Eq. 1 neglecting the frictions:

$$\tau = M(q)\ddot{q} + C(q,\dot{q}) + G(q) \tag{1}$$

where, q is joint angles of the exoskeleton, M is a 3×3 inertia matrix, C is a 3×3 vector of nonlinear Coriolis forces and centripetal forces, G is a 3×1 vector of gravity and τ is a 3×1 vector of the control input torques. The elements in the M, C and G consist of the inertia parameters of each link which is a vector of ten constant values (the mass of link, the moment of inertia, the product of inertia and the center of gravity to the coordinate) as in Eq. 2:
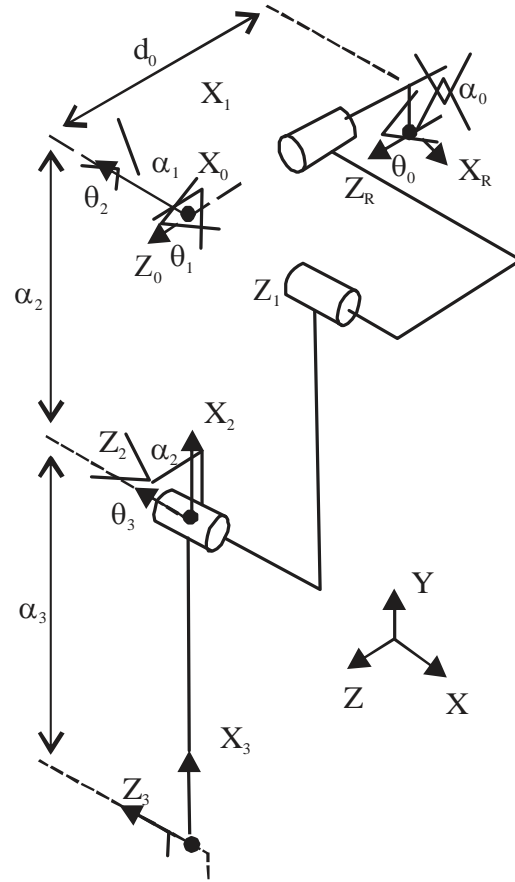

Fig. 3: Coordinate translate relations of the exoskeleton

Table 1: D-H parameters of exoskeleton robot

0	90°	d_0	a_0	0
1	q_1	0	0	-90°
2	q_2	0	a_2	0
3	q_3	0	a_3	0

$$F_i = [m_i, I_{xx,i}, I_{yy,i}, I_{zz,i}, I_{xy,i}, I_{xz,i}, I_{yz,i}, x_i, y_i, z_i](i = 1, 2, 3) \tag{2}$$

where, m_i is the mass of link i, $I_{xx,i}$, $I_{yy,i}$, $I_{zz,i}$ are the moment of inertia respected to the coordinate {i}, $I_{xy,i}$, $I_{xz,i}$, $I_{yz,i}$ are the product of inertia respected to the coordinate {I}, x_i, y_i, z_i are the coordinate value of the link's mass centre.

Put the inertia constant values defined by Eq. 2 into the exoskeleton dynamics defined in Eq. 1, the linear form of the exoskeleton's dynamic model can be derived as in Eq. 3:

$$\Phi_{exo}(q_{exo}, \dot{q}_{exo}, \ddot{q}_{exo})P_{exo} = \tau_{exo} \tag{3}$$

where, τ_{exo} is a 3×1 vector, which represents the joint torques of the exoskeleton, Φ_{exo} is a 3×19 regressed

variable matrix and P_{exo} is a 19×1 vector that is the unknown inertia parameters of the exoskeleton dynamic model. The elements in Φ_{exo} and P_{exo} are defined in the appendix:

$\Phi_{1,1}^{exo} = \ddot{q}_1$

$\Phi_{1,2} = \ddot{q}_1(\cos(2q_2 + q_3) + \cos(q_3)) - (2\dot{q}_1\dot{q}_2 + \dot{q}_1\dot{q}_3)\sin(2q_2 + q_3)$
$\qquad - \dot{q}_1\dot{q}_3\sin(q_3)$

$\Phi_{1,3} = \ddot{q}_1\cos(2q_2) - 2\dot{q}_1\dot{q}_2\sin(2q_2)$

$\Phi_{1,4} = \ddot{q}_1(\sin(2q_2 + q_3) + \sin(q_3)) + (2\dot{q}_1\dot{q}_2 + \dot{q}_1\dot{q}_3)\cos(2q_2 + q_3)$
$\qquad + \dot{q}_1\dot{q}_3\cos(q_3)$

$\Phi_{1,5} = \ddot{q}_1\sin(2q_2) + 2\dot{q}_1\dot{q}_2\cos(2q_2)$

$\Phi_{1,6} = \ddot{q}_1\cos(2q_2 + 2q_3) - 2(\dot{q}_1\dot{q}_2 + \dot{q}_1\dot{q}_3)\sin(2q_2 + 2q_3)$

$\Phi_{1,7} = \ddot{q}_1\sin(2q_2 + 2q_3) + 2(\dot{q}_1\dot{q}_2 + \dot{q}_1\dot{q}_3)\cos(2q_2 + 2q_3)$

$\Phi_{1,8} = (\ddot{q}_2 + \ddot{q}_3)\sin(q_2 + q_3) + (\dot{q}_2 + \dot{q}_3)^2\cos(q_2 + q_3)$

$\Phi_{1,9} = (\ddot{q}_2 + \ddot{q}_3)\cos(q_2 + q_3) - (\dot{q}_2 + \dot{q}_3)^2\sin(q_2 + q_3)$

$\Phi_{1,10} = \Phi_{1,19} = \sin(q_1)\sin(q_2 + q_3)$

$\Phi_{1,11} = \ddot{q}_2\sin(q_2) + \dot{q}_2^2\cos(q_2)$

$\Phi_{1,14} = \cos(q_1)$

$\Phi_{1,15} = \sin(q_1)$

$\Phi_{1,16} = \cos(q_2)\sin(q_1)$

$\Phi_{1,17} = \sin(q_1)\sin(q_2)$

$\Phi_{1,18} = \sin(q_1)\cos(q_2 + q_3)$

$\Phi_{2,2} = (2\ddot{q}_2 + \ddot{q}_3)\cos(q_3) + \dot{q}_1^2\sin(2q_2 + q_3) - \dot{q}_3(2\dot{q}_2 + \dot{q}_3)\sin(q_3)$

$\Phi_{2,3} = \dot{q}_1^2\sin(2q_2)$

$\Phi_{2,4} = (2\ddot{q}_2 + \ddot{q}_3)\sin(q_3) - \dot{q}_1^2\cos(2q_2 + q_3) + \dot{q}_3(2\dot{q}_2 + \dot{q}_3)\cos(q_3)$

$\Phi_{2,5} = -\dot{q}_1^2\cos(2q_2)$

$\Phi_{2,6} = \Phi_{3,6} = \dot{q}_1^2\sin(2q_2 + 2q_3)$

$\Phi_{2,7} = \Phi_{3,7} = -\dot{q}_1^2\cos(2q_2 + 2q_3)$

$\Phi_{2,8} = \Phi_{3,8} = \ddot{q}_1\sin(q_2 + q_3)$

$\Phi_{2,9} = \Phi_{3,9} = \ddot{q}_1\cos(q_2 + q_3)$

$\Phi_{2,10} = \Phi_{2,19} = \Phi_{3,10} = \Phi_{319} = -\cos(q_1)\cos(q_2 + q_3)$

$\Phi_{2,11} = \ddot{q}_1\sin(q_2)$

$\Phi_{2,12} = \ddot{q}_2$

$\Phi_{2,13} = \ddot{q}_3$

$\Phi_{2,16} = \cos(q_1)\sin(q_2)$

$\Phi_{2,17} = -\cos(q_1)\cos(q_2)$

$\Phi_{2,18} = \Phi_{3,18} = \cos(q_1)\sin(q_2 + q_3)$

$\Phi_{3,2} = \ddot{q}_2\cos(q_3) + \dot{q}_1^2\sin(2q_2 + q_3)/2 + (\dot{q}_1^2 + 2\dot{q}_2^2)\sin(q_3)/2$

$\Phi_{3,4} = \ddot{q}_2\sin(q_3) - \dot{q}_1^2\cos(2q_2 + q_3)/2 - (\dot{q}_1^2 + 2\dot{q}_2^2)\cos(q_3)/2$

$\Phi_{3,13} = \ddot{q}_2 + \ddot{q}_3$

$\Phi_{1,12} = \Phi_{1,13} = \Phi_{2,1} = \Phi_{2,14} = \Phi_{2,15} = 0$

$\Phi_{3,1} = \Phi_{3,3} = \Phi_{3,5} = \Phi_{3,11} = \Phi_{3,12} = \Phi_{3,14} = \Phi_{3,15} = \Phi_{3,16} = \Phi_{3,17} = 0$

$P_{exo} = 0.5(I_{2xx} + I_{3xx} + 2I_{1yy} + I_{2yy} + I_{3yy}) + 0.5a_2^2m_2 + 0.5(a_2^2 + a_3^2)m_3$
$\qquad + a_2m_2r_{2x} + a_3m_3r_{3x}$

$P_2 = a_2a_3m_3 + a_2m_3r_{3x};$

$P_3 = -0.5I_{2xx} + 0.5I_{2yy} + 0.5a_2^2(m_2 + m_3) + a_2m_2r_{2x}$

$P_4 = -a_2m_3r_{3y}$

$P_5 = -I_{2xy} - a_2m_2r_{2y}$

$P_6 = -0.5I_{3xx} + 0.5I_{3yy} + 0.5a_3^2m_3 + a_3m_3r_{3x}$

$P_7 = -a_3m_3r_{3y} - I_{3xy}$

$P_8 = I_{3xz} + a_3m_3r_{3z}$

$P_9 = I_{3yz}$

$P_{10} = I_{2yz}$

$P_{11} = I_{2xz} + a_2(m_2r_{2z} + m_3r_{3z})$

$P_{12} = I_{2zz} + I_{3zz} + a_2^2m_2 + (a_2^2 + a_3^2)m_3 + 2a_2m_2r_{2x} + 2a_3m_3r_{3x}$

Upper limb dynamics modeling: The dynamic model of the upper limb can be derived as Eq. 4:

$$\Phi_u(q_u, \dot{q}_u, \ddot{q}_u)P_u = \tau_u \tag{4}$$

where, τ_u is a 3×1 vector, which represents the joint torques of the upper limb, Φ_u is a 3×19 regressed variable matrix and P_u is a 19×1 vector that is the unknown inertia parameters of the upper limb dynamic model. The dynamics of the upper limb and the exoskeleton have the same structure but different parameters. Besides the shoulder elevation degree of freedom has no links; in other words, the inertia parameter of link 1, F_1 is zero. The elements in Φ_u and P_u can also be listed separately.

Modeling and simulation of human-computer interaction dynamics: The schematic of the human-computer interaction model is shown in Fig. 4. It can be seen that the exoskeleton is wearied on the upper limb and support the upper limb. Both the exoskeleton and HUL can be regarded as a robot with three degrees of freedom as the wrist joints have been neglected. The length of the exoskeleton can be adjusted, so the joint rotation centres can be in the same axis. As a result, they have the same kinematics and Jacobian matrix, the structures of the dynamics are same but the parameters are different. The interaction dynamic model of the human-exoskeleton is established by combining the dynamics of HUL and the exoskeleton.

Human-computer interaction dynamics modeling: Combining the exoskeleton dynamic model and the upper limb dynamic model[20], the human-computer dynamic model can be derived as Eq. 5:

$$J_{exo}^T J_u^{-T}\Phi_u(q_u, \dot{q}_u, \ddot{q}_u)P_u + \Phi_{exo}(q_{exo}, \dot{q}_{exo}, \ddot{q}_{exo})P_{exo} = \tau_m \tag{5}$$
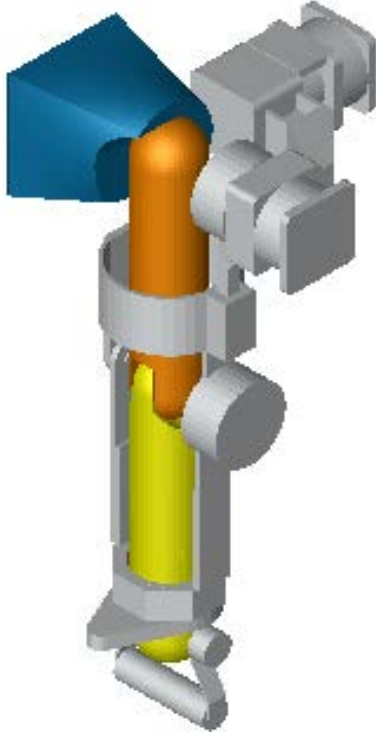
Fig. 4: Schematic of the human-computer interaction model

where, t_m is the combined joint torques of the exoskeleton and the upper limb, it is the values that can be measured by the torque sensors mounted on the exoskeleton joints and J_{exo}^T and J_u are the Jacobian matrix, respectively of the exoskeleton and the upper limb as is shown in Eq. 6:

$$J_{exo} = \begin{bmatrix} J_{1,1}^{exo} & J_{1,2}^{exo} & J_{1,3}^{exo} \\ J_{2,1}^{exo} & J_{2,2}^{exo} & J_{2,3}^{exo} \\ J_{3,1}^{exo} & J_{3,2}^{exo} & J_{3,3}^{exo} \\ J_{4,1}^{exo} & J_{4,2}^{exo} & J_{4,3}^{exo} \\ J_{5,1}^{exo} & J_{5,2}^{exo} & J_{5,3}^{exo} \\ J_{6,1}^{exo} & J_{6,2}^{exo} & J_{6,3}^{exo} \end{bmatrix} \quad J_u = \begin{bmatrix} J_{1,1}^{u} & J_{1,2}^{u} & J_{1,3}^{u} \\ J_{2,1}^{u} & J_{2,2}^{u} & J_{2,3}^{u} \\ J_{3,1}^{u} & J_{3,2}^{u} & J_{3,3}^{u} \\ J_{4,1}^{u} & J_{4,2}^{u} & J_{4,3}^{u} \\ J_{5,1}^{u} & J_{5,2}^{u} & J_{5,3}^{u} \\ J_{6,1}^{u} & J_{6,2}^{u} & J_{6,3}^{u} \end{bmatrix} \quad (6)$$

Where:

$$J_{1,1}^{exo} = -\cos(q_1)(a_2^{exo}\cos(q_2) + a_3^{exo}\cos(q_2 + q_3))$$

$$J_{1,2}^{exo} = \sin(q_1)(a_2^{exo}\sin(q_2) + a_3^{exo}\sin(q_2 + q_3))$$

$$J_{1,3}^{exo} = a_3^{exo}\sin(q_1)\sin(q_2 + q_3)$$

$$J_{2,1}^{exo} = -\sin(q_1)(a_2^{exo}\cos(q_2) + a_3^{exo}\cos(q_2 + q_3))$$

$$J_{2,2}^{exo} = -\cos(q_1)(a_2^{exo}\sin(q_2) + a_3^{exo}\sin(q_2 + q_3))$$

$$J_{2,3}^{exo} = -a_3^{exo}\cos(q_1)\sin(q_2 + q_3)$$

$$J_{3,1}^{exo} = 0$$

$$J_{3,2}^{exo} = -a_2^{exo}\cos(q_2) - a_3^{exo}\cos(q_2 + q_3)$$

$$J_{3,3}^{exo} = -a_3^{exo}\cos(q_2 + q_3)$$

$$J_{4,1}^{exo} = 0$$

$$J_{4,2}^{exo} = -\cos(q_1)$$

$$J_{4,3}^{exo} = -\cos(q_1)$$

$$J_{5,1}^{exo} = 0$$

$$J_{5,2}^{exo} = -\sin(q_1)$$

$$J_{5,3}^{exo} = -\sin(q_1)$$

$$J_{6,1}^{exo} = 1$$

$$J_{6,2}^{exo} = 0$$

$$J_{6,3}^{exo} = 0$$

$$J_{1,1}^{u} = -\cos(q_1)(a_2^{u}\cos(q_2) + a_3^{u}\cos(q_2 + q_3))$$

$$J_{1,2}^{u} = \sin(q_1)(a_2^{u}\sin(q_2) + a_3^{u}\sin(q_2 + q_3))$$

$$J_{1,3}^{u} = a_3^{u}\sin(q_1)\sin(q_2 + q_3)$$

$$J_{2,1}^{u} = -\sin(q_1)(a_2^{u}\cos(q_2) + a_3^{u}\cos(q_2 + q_3))$$

$$J_{2,2}^{u} = -\cos(q_1)(a_2^{u}\sin(q_2) + a_3^{u}\sin(q_2 + q_3))$$

$$J_{2,3}^{u} = -a_3^{u}\cos(q_1)\sin(q_2 + q_3)$$

$$J_{3,1}^{u} = 0$$

$$J_{3,2}^{u} = -a_2^{u}\cos(q_2) - a_3^{u}\cos(q_2 + q_3)$$

$$J_{3,3}^{u} = -a_3^{u}\cos(q_2 + q_3)$$

$$J_{4,1}^{u} = 0$$

$$J_{4,2}^{u} = -\cos(q_1)$$

$$J_{4,3}^{u} = -\cos(q_1)$$

$$J_{5,1}^{u} = 0$$

$$J_{5,2}^{u} = -\sin(q_1)$$

$$J_{5,3}^{u} = -\sin(q_1)$$

$$J_{6,1}^{u} = 1$$

$$J_{6,2}^{u} = 0$$

$$J_{6,3}^{u} = 0$$

As mentioned above, because of the adjusted links, the exoskeleton and the upper limb have the same kinematics. $J_{exo} = J_u$ and $\Phi_u = \Phi_{exo}$ in this study. The Eq. 6 can be arranged as follows:

$$(q, \dot{q}, \ddot{q})P = \tau_m$$
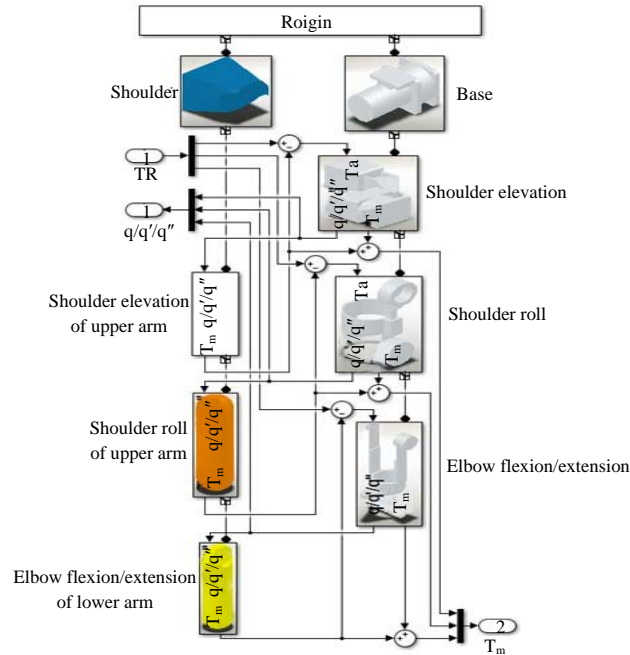$$P = P_u = P_{exo} \quad (7)$$

Fig. 5: Simulink model of the human-computer interaction dynamics

Where:

$$\Phi = \Phi_u = \Phi_{exo} \text{ and } P = P_u = P_{exo}$$

In order to validate it in the simulation, it has been written in the form of state function as Eq. 8:

$$\ddot{q} = M(q,P)^{-1}(\tau_m - C(q,\dot{q},P)\dot{q} - G(q,P)) \tag{8}$$

$C = [-P_6(dq_2+dq_3)\sin(2q_2+2q_3)+P_4dq_3/2\cos(q_3)$
$\quad +P_7(dq_2+dq_3)\cos(2q_2+2q_3)-P_2dq_3/2\sin(q_3)$
$\quad +P_4(dq_2+dq_3/2)\cos(2q_2+q_3)-P_2(dq_2+dq_3/2)\sin(2q_2+q_3)$
$\quad +P_5dq_2\cos(2q_2)-P_3dq_2\sin(2q_2),-P_6dq_1\sin(2q_2+2q_3)+P_{11}dq_2\cos(q_2)$
$\quad +P_7dq_1\cos(2q_2+2q_3)+P_4dq_1\cos(2q_2+q_3)-P_2dq_1\sin(2q_2+q_3)$
$\quad +P_5dq_1\cos(2q_2)-P_3dq_1\sin(2q_2)+P_8(dq_2+dq_3)\cos(q_2+q_3)$
$\quad -P_9(dq_2+dq_3)\sin(q_2+q_3)-P_{10}dq_2\sin(q_2),-P_6dq_1\sin(2q_2+2q_3)$
$\quad +P_4dq_1/2\cos(q_3)+P_7dq_1\cos(2q_2+2q_3)-P_2dq_1/2\sin(q_3)$
$\quad +P_4dq_1/2\cos(2q_2+q_3)-P_2dq_1/2\sin(2q_2+q_3)+P_8(dq_2+dq_3)\cos(q_2+q_3)$
$\quad -P_9(dq_2+dq_3)\sin(q_2+q_3);dq_1(-P_4\cos(2q_2+q_3)-P_5\cos(2q_2)$
$\quad +P_2\sin(2q_2+q_3)+P3\sin(2q_2)-P_7\cos(2q_2+2q_3)+P_6\sin(2q_2+2q_3)),$
$\quad dq_3(P_4\cos(q_3)-P_2\sin(q_3)),(dq_2+dq_3)(P_4\cos(q_3)-P_2\sin(q_3));$
$\quad dq_1(-P_4/2\cos(2q_2+q_3)+P_2/2\sin(2q_2+q_3)-P_7\cos(2q_2+2q_3)$
$\quad +P_6\sin(2q_2+2q_3)-P_4/2\cos(q_3)+P_2/2\sin(q_3)),$
$\quad -dq_2(P_4\cos(q_3)-P_2\sin(q_3)),0]$

$M = [P_1 + P_2(\cos(2q_2 + q_3) + \cos(q_3)) + P_3\cos(2q_2) + P_4(\sin(2q_2 + q_3) + \sin(q_3))$
$\quad +P_5\sin(2q_2) + P_6\cos(2q_2 + 2q_3) + P_7\sin(2q_2 + 2q_3)P_8\sin(q_2 + q_3) + P_9\cos(q_2 + q_3)$
$\quad +P_{10}\cos(q_2) + P_{11}\sin(q_2), P_8\sin(q_2 + q_3) + P_9\cos(q_2 + q_3); P_8\sin(q_2 + q_3)$

$\quad +P_9\cos(q_2 + q_3) + P_{10}\cos(q_2) + P_{11}\sin(q_2), P_{12} + 2P_2\cos(q_3) + 2P_4\sin(q_3), P_{13}$
$\quad +P_2\cos(q_3) + P_4\sin(q_3); P_8\sin(q_2 + q_3) + P_9\cos(q_2 + q_3), P_{13} + P_2\cos(q_3) + P_4\sin(q3), P_{13}]$

$G = [P_{14}\cos(q_1) + P_{15}\sin(q_1) + P_{16}\sin(q_1)\cos(q_2) + P_{17}\sin(q_1)\sin(q_2)$
$\quad +P_{18}(\cos(q_2)\cos(q_3) - \sin(q_2)\sin(q_3))\sin(q_1)$
$\quad +P_{19}\sin(q_1)(\sin(q_2)\cos(q_3) + \sin(q_3)\cos(q_2))$
$\quad \cos(q_1)(-P_{19}\cos(q_2 + q_3) + P_{18}\sin(q_2 + q_3) - P_{17}\cos(q_2) + P_{16}\sin(q_2))$
$\quad \cos(q_1)(-P_{19}\cos(q_2 + q_3) + P_{18}\sin(q_2 + q_3))]$

Simulation modeling of human-computer interaction dynamics: Ignoring the effect of the little parts and retaining the structure characters, the prototype of the human-computer interaction can be drawn out using the SolidWorks as has shown in Fig. 4. Then the prototype is translated into the Simulink model of the exoskeleton and HUL by Simulink/SimMechanics[21]. The measured joint torques is the result of adding the two model's joint torques. Then we get human-computer interaction Simulink model after the input and output had been set. Thanks to the subsystem packaging technology, the Simulink model of the human-computer interaction dynamics looks nice and well-formed as is shown in Fig. 5.

where, TR is the input torque of system, T_m is the torque value measured by the torque sensors mounted on the joint of the exoskeleton, q/q'/q" is the motion state of the system.
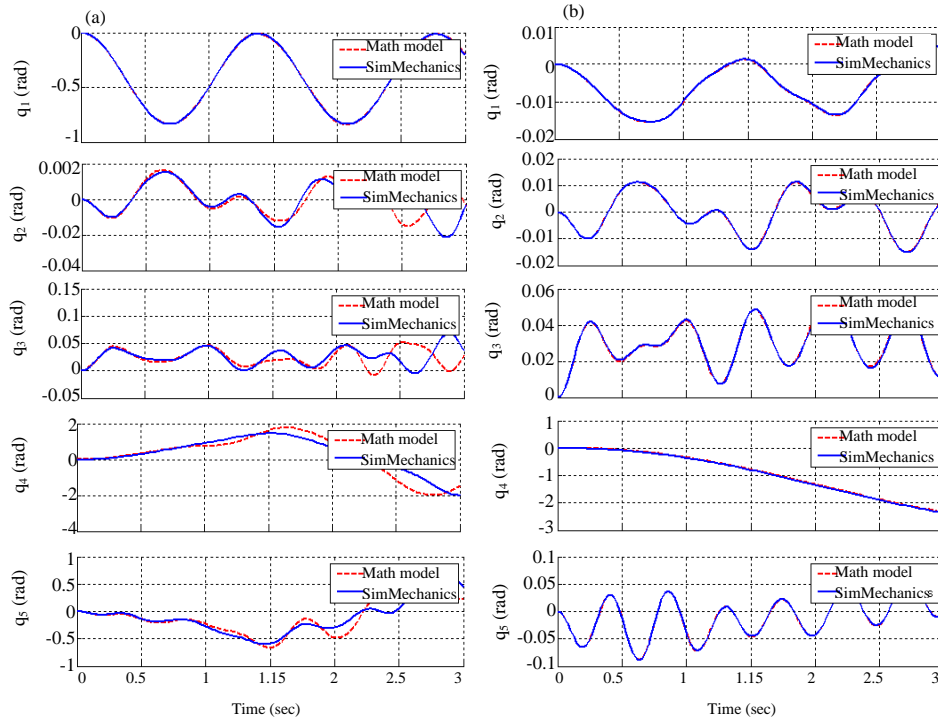
Fig. 6(a-b): Simulation results of the math model and the SimMechanics model

RESULTS

The accuracy of the human-computer interaction dynamics can be verified by comparing the joint motion response of the math model and Simulink model with the same input torques. The zero state zero input and the zero state specific input experience are proceed on the math model (described in Eq. 8) and the Simulink model (depicted in Fig. 5), respectively. Observe and compare the two model's response and verify the accuracy of the human-computer interaction dynamics.

Simulation experience: The parameters P of human-computer interaction dynamics are listed in Table 2. Establish a system function in the MATLAB based on the Eq. 8 and the parameters in Table 2. Compare the response of the math model to the results of the SimMechanics model in the Simulink environment. The simulation time is set as 5 sec.

Figure 6 depicts the simulation results of the math model and the SimMechanics model. A is the zero state zero input response and B is the response with input $\tau = [12\ 2\ 2]^T$. Obviously, the difference of the simulation results of math model and the SimMechanics model is really small and it can be seen that the output has a nonlinear relationship to the

Table 2: Parameters P of human-computer interaction dynamics

P_{Exo}	P_u	$P (P_{Exo} + P_u)$
0.2801161255506	0.1147375572134	0.394853682764
0.1201880879334	0.0771360313344	0.1973241192678
0.1209970452548	0.0792509021856	0.2002479474404
-0.0029055675672	0	-0.0029055675672
-1.3465e-07	7.88275008e-05	0.0000786928508
0.0606278698858	0.0330495630078	0.0936774328936
-0.0034822801664	0	-0.0034822801664
0.0185659802897	0	0.0185659802897
-1.884e-08	2.472e-08	0.00000000588
1.0244e-07	-6.7e-10	0.00000010177
0.0706665739311	7.4e-10	0.0706665746711
0.3710739750212	0.2270482770568	0.598122252078
0.1248840267216	0.0673920404456	0.1922760671672
6.145028964135001	0	6.145028964135001
-3.99473991e-04	0	-0.000399473991
9.106594966944002	6.220828767168	15.327423734112003
0	0.002510088624	0.002510088624
4.256480659302	2.731785080832	6.988265740134001
-0.102901147416	0	-0.102901147416

input, they are coupled on the state. In a word, the human-computer interaction dynamics model in this study can reflect the torque and motion relationship between the exoskeleton and HUL. This model is a nonlinear coupled system with multivariable.

In a practical application, the human motion desire can be recognized by comparing the estimated torques to the measured torques based on the Eq. 7. It will improve the active rehabilitation exercises.

DISCUSSION

Active exercise rehabilitation training is the necessary process during the upper limb rehabilitation training. How accurately determine the desire of human motion using the rehabilitation system, it makes the study more and more precise.

The dynamic modeling of exoskeleton upper limb rehabilitation robot is generally considered the robot mechanical arm model for convenience only. Human upper limb dynamic model is considered in this study, which overcomes the problem of model inaccuracy and determines patient movement intentions.

The combined model of this study called human-computer interaction dynamic model, which consist of robot mechanical arm model and human upper limb model has solved the problem of human motion's desire, which unable to determine by mathematical model.

Compare with Newton-Euler method[22], Kane equation method[23] and other robot modeling methods, robot mechanical arm dynamic model of this study gives a Lagrange dynamic equation with 19 parameters based on the pseudo inertia matrix; in addition, it has nothing to do with unknown constraining force.

Human upper limb dynamic model[24] of this study is considered, which is taken as two links with three degrees of freedom and it is the best way for the human-computer system control.

The effects of combined model are discussed: On the one hand, the control accuracy of the combined model is higher, the performance is better; on the other hand, it can accurately determine patient movement intentions.

The characteristic rule and physical components are combined to establish 3D dynamic model for upper-limb rehabilitation robot by using simmechanics software and simulink software. The 3D dynamic model show the running processes of upper-limb rehabilitation robot directly and actually by visual simulation in the virtual reality environment.

CONCLUSION

Considering interference and uncertain factors of external equipment, this article accurately determines patient movement intentions by model. It has modeled the human-computer interaction dynamics to recognize the human motion desire in time for the purpose of the active rehabilitation exercises which have been proven effective to the patients with upper limb dysfunctions.

It is important to do upper-limb rehabilitation training by using rehabilitation robot in rehabilitation engineering and this is a very meaningful study. Future study will focus on the application of human-computer interaction dynamic model which had been obtained in this study.

The Graphical programming virtual platform for upper-limb rehabilitation robot system is a integrated environment based on graphical developing, debugging and running. It laid the foundation for rehabilitation evaluation and discusses the application of computer software technology in rehabilitation medicine.

ACKNOWLEDGMENT

REFERENCES

1. Norouzi-Gheidari, N., P.S. Archambault and J. Fung, 2012. Effects of robot-assisted therapy on stroke rehabilitation in upper limbs: Systematic review and meta-analysis of the literature. J. Rehabil. Res. Dev., 49: 479-496.

2. He, W. and K. Wang, 2014. Advance in rehabilitation of upper limb function in hemiplegic patients after stroke (review). China J. Rehabil. Theory Pract., 20: 334-339.

3. Connell, L.A., N.E. Mcmahon, J.E. Harris, C.L. Watkins and J.J. Eng, 2014. A formative evaluation of the implementation of an upper limb stroke rehabilitation intervention in clinical practice: A qualitative interview study. Implementation Sci., Vol. 9. 10.1186/s13012-014-0090-3

4. Xia, B., Z. Wu and H.Y. Liu, 2014. Clinical research on upper limb rehabilitation robot for upper limb movement function in patients with hemiplegia therapy. Chin. J. Pract. Nervous Dis., 17: 104-106.

5. Fazekas, G., M. Horvath, T. Troznai and A. Toth, 2007. Robot-mediated upper limb physiotherapy for patients with spastic hemiparesis: A preliminary study. J. Rehabil. Med., 39: 580-582.

6. Kwakkel, G., B.J. Kollen and H.I. Krebs, 2008. Effects of robot-assisted therapy on upper limb recovery after stroke: A systematic review. Neurorehabilitation Neural Repair, 22: 111-121.

7. Lo, H.S. and S.Q. Xie, 2012. Exoskeleton robots for upper-limb rehabilitation: State of the art and future prospects. Med. Eng. Phys., 34: 261-268.

8. Frisoli, A., E. Sotgiu, C. Procopio, M. Bergamasco, B. Rossi and C. Chisari, 2011. Design and implementation of a training strategy in chronic stroke with an arm robotic exoskeleton. Proceedings of the IEEE International Conference on Rehabilitation Robotics, June 29-July 1, 2011, Zurich, pp: 1-8.

9. Ren, Y.P., S.H. Kang, H.S. Park, Y.N. Wu and L.Q. Zhang, 2013. Developing a multi-joint upper limb exoskeleton robot for diagnosis, therapy and outcome evaluation in neurorehabilitation. IEEE Trans. Neural Syst. Rehabil. Eng., 21: 490-499.

10. Li, Q.L., T.M. Ye, Z.J. Du, L.N. Sun and D.Y. Wang, 2009. Controlled assistance by an exoskeletal rehabilitation robot for upper limbs. J. Harbin Eng. Univ., 30: 166-170.

11. Wang, D.Y., Q.L. Li, Z.J. Du and L.N. Sun, 2007. Study on exoskeletal rehabilitation robot for upper limb and its control method. J. Harbin Eng. Univ., 28: 1008-1013.

12. Li, X., J.H. Wang and X.K. Fang, 2012. Dynamic modeling and simulation of 5-DOF upper-limb rehabilitation robot. Control Eng. China, 19: 823-831.

13. Niku, S., 2011. Introduction to Robotics: Analysis, Control, Applications. 2nd Edn., Wiley India Pvt. Ltd., New Delhi, India, pp: 112-134.

14. Rahman, M.H., C. Ochoa-Luna, M.J. Rahman, M. Saad and P. Archambault, 2014. Force-position control of a robotic exoskeleton to provide upper extremity movement assistance. Int. J. Mod. Identificat. Control, 21: 390-400.

15. Yang, Q.Z., D.F. Cao and J.H. Zhao, 2013. Analysis on state of the art of upper limb rehabilitation robots. Robot, 35: 630-640.

16. Amsuss, S., P.M. Goebel, N. Jiang, B. Graimann, L. Paredes and D. Farina, 2014. Self-correcting pattern recognition system of surface EMG signals for upper limb prosthesis control. IEEE Trans. Biomed. Eng., 61: 1167-1176.

17. Li, Z., B. Wang, F. Sun, C. Yang, Q. Xie and W. Zhang, 2014. sEMG-based joint force control for an upper-limb power-assist exoskeleton robot. IEEE J. Biomed. Health Inform., 18: 1043-1050.

18. Bi, Q. and C.J. Yang, 2014. Human-machine interaction force control: Using a model-referenced adaptive impedance device to control an index finger exoskeleton. J. Zhejiang Univ. Sci. C, 15: 275-283.

19. Frisoli, A., C. Procopio, C. Chisari, I. Creatini and L. Bonfiglio *et al*., 2012. Positive effects of robotic exoskeleton training of upper limb reaching movements after stroke. J. NeuroEng. Rehabil., Vol. 9. 10.1186/1743-0003-9-36

20. Wang, W., Z.G. Hou, L. Tong, Y. Chen, L. Peng and M. Tan, 2014. Dynamics modeling and identification of the human-robot interface based on a lower limb rehabilitation robot. Proceedings of the 2014 IEEE International Conference on Robotics and Automation (ICRA), May 31-June 7, 2014, Hong Kong, pp: 6012-6017.

21. Wang, J., Z. Jiang, X. Wang, Y. Zhang and D. Guo, 2011. Kinematics simulation of upper limb rehabilitant robot based on virtual reality techniques. Proceedings of the 2011 2nd International Conference on Artificial Intelligence, Management Science and Electronic Commerce (AIMSEC), August 8-10, 2011, Deng Leng, pp: 6681-6683.

22. Hwang, Y.L. and V.T. Truong, 2015. Dynamic analysis and control of multi-body manufacturing systems based on newton-euler formulation. Int. J. Comput. Methods. 10.1142/S0219876215500073

23. Chopik, A.V., K.Y. Shtivel'man, P.M. Gritsyuk and O.Y. Bazyuk, 1994. Kane equation for deformed diamond-like crys-talline semiconductors. Russian Phys. J., 37: 677-681.

24. Masinghe, W., G. Collier, A. Ordys and T. Nanayakkara, 2012. A novel approach to determine the inverse kinematics of a human upper limb model with 9 degrees of freedom. Proceedings of the 2012 IEEE EMBS Conference on Biomedical Engineering and Sciences (IECBES), December 17-19, 2012, Langkawi, pp: 525-530.